Preparation of novel silica structures using a library of carbohydrate gel assemblies as templates for sol–gel transcription

Jong Hwa Jung,† Masato Amaike, Kazuaki Nakashima and Seiji Shinkai *

Chemotransfiguration Project, Japan Science and Technology Corporation (JST), 2432 Aikawa, Kurume, Fukuoka, 839-0861, Japan. E-mail: seijitcm@mbox.nc.kyushu-u.ac.jp; Fax: +81 942 39 9012

Received (in Cambridge, UK) 14th May 2001, Accepted 19th July 2001
First published as an Advance Article on the web 7th September 2001

Four sugar-based organogelators (**1**–**4**) were synthesized, and their gelation ability was evaluated in organic solvents and water. It was shown that they act as versatile gelators of various organic fluids, forming various superstructural aggregates. The xerogels showed a single- and lotus-type fiber structure or a spherical structure. The difference in these organogel supramolecular structures has successfully been transcribed into silica structures by sol–gel polycondensation of tetraethoxysilane (TEOS), resulting in single or multiple (lotus-shaped) hollow fiber structures with 5–10 nm inner diameters or a spherical structure with 700–1300 nm outer diameters. These results indicate that novel silica structures can be created by transcription of various superstructures formed in organogels through the hydrogen-bonding interaction. Nitrogen adsorption–desorption isotherms were measured by a BET method. The silica obtained from the α-glucose-based organogel **1**, β-glucose-based organogel **2**, α-galactose-based organogel **3** and α-mannose-based organogel **4** had BET surface areas of 450, 475, 650 and 670 $m^2\ g^{-1}$, respectively. The Q^4/Q^3 ratios of these silicas were estimated by ^{29}Si MAS NMR spectroscopy. The Q^4/Q^3 ratios for the silica materials obtained from **1**, **2**, **3** and **4** were 3.00, 3.05, 4.87 and 5.25, respectively. This is a novel and successful example showing that a variety of new silica structures are created using a library of carbohydrate gel fibers as their templates.

Introduction

The use of organic molecules, assemblies and supramolecular systems in the development of novel materials continues to offer new and exciting alternatives to conventional synthetic strategies.[1] Since these higher-order aggregates can provide various architectures, sol–gel polycondensation utilizing them as templates results in various novel architectures which cannot be created directly from inorganic materials. For example, block copolymer lyotropic mesophases,[2a] latex particles,[2b] colloidal crystals,[2c] filamentous crystals[2d] and gelators[2e,f] have been employed in the synthesis of novel inorganic–organic composites with controlled size, shape, organization and porosity. Such materials could have important applications in separation and purification processes, catalysis, storage and release systems, smart fillers and quantum devices.

Our current research purpose is to utilize the superstructural aggregates constructed in the organogel systems as templates for sol–gel polycondensation. The gelators can be classified into two categories according to the driving force for molecular aggregation: non-hydrogen-bond-based gelators and hydrogen-bond gelators. Typical examples of the former are cholesterol derivatives.[3] Typical examples of the latter are amide-,[4a–c] urea-based cyclohexanediamines[4d] and sugar-based gelators.[4e] In particular, cholesterol-based organogel templates have created various hollow silica fibers with linear,[5a,b] helical[5c] and multi-layered structures[5d,e] by sol–gel polycondensation. The findings indicate that the cholesterol-based organogel fibers act as an efficient template to create an inside tube in the polycondensation process. It is already known that either the cationic charge or the efficient hydrogen-bonding site is indispensable to the sol–gel transcription in order to adsorb 'anionic' silica particles onto the organic molecular assemblies.[5,6] Meanwhile, the sugar-based gelators provide various, morphologically-novel superstructures such as linear,[7] helical,[7,8] bundled,[8a] multi-layered cigar-like[8b] and vesicular[8b] structures depending on their self-assembling manner in the gel phase. Despite their structural variety, however, the transcription of sugar-integrated organogel structure into the silica structure is unprecedented, because introduction of a moderate amount of cationic charge into the organogelator is very difficult and the gelation ability is remarkably reduced in the protic sol–gel medium required for sol–gel polycondensation. To overcome this dilemma, we designed the sugar-based organogelators **1**–**4** in which the amino group not only stabilizes the organogels due to the intensified inter-gelator hydrogen bonds[7] but also binds tetraethoxysilane (TEOS) through the hydrogen-bonding interaction.[6a–c]

One purpose of this work is to obtain novel silica with a variety of morphologies using a library of the sugar-based gelators. Another purpose is to fix various novel organic superstructures created by weak intermolecular forces as permanent structures in inorganic materials. This is usually achieved by 'physical' methods such as changing the pH of the initial surfactant solution,[9a] or changing the surfactant hydrophobicity.[9a] For example, morphological studies have revealed that macroscopic precipitates consisting of hexagonally ordered silica show noncrystallographic symmetry including gyroids, helicoils and curved tubules.[9] As an alternate method, we here offer a 'chemical' method: that is, we have found that the novel morphologies of the sugar-based gelators are successfully transcribed into the silica prepared under the specific sol–gel polycondensation conditions. The present paper reports the full achievement of the creation of various new silica structures using the sugar-based gelators as templates.

† *Present address*: CREST, Japan Science and Technology Corporation (JST), Nanoarchitectonics Research Center, National Institute of Advanced Industrial Science and Technology (AIST), Tsukuba Central 4, 1-1-1 Higashi, Tsukuba, Ibaraki 305-8562, Japan.

 DOI: 10.1039/b104190h

Table 1 Gelation ability of **1**–**4**[a] in organic solvents

Solvent	Gelator			
	1	**2**	**3**	**4**
Hexane	I	I	I	I
Carbon tetrachloride	I	I	I	I
Benzene	I	I	I	I
Chloroform	G	I	I	I
Ethyl acetate	G	I	R	I
Methanol	G	S	G	G
Ethanol	G	G	G	G
Propan-1-ol	G	G	R	R
Butan-1-ol	G	G	R	R
Acetic acid	S	S	S	G
Water	G	R	G	G

[a] Gelator = 3.0 wt%; G = stable gel, S = solution, R = precipitation, I = insoluble.

Results and discussion

Gelation ability and transmission electron microscopy (TEM) observations of xerogels

Compounds **1**–**4** were synthesized according to Scheme 1. Compounds **5**–**8** were prepared by treatment of the corresponding saccharides with benzaldehyde and $ZnCl_2$, and reduced with H_2 and Pd on charcoal to give the desired products. The products were identified by ^1H NMR, IR and MS spectral evidence and elemental analyses. The gelation ability of these gelators **1**–**4** was estimated in organic solvents and water. The results are summarized in Table 1. It is seen from Table 1 that these gelators can gelate 3–7 out of 11 organic solvents. More interestingly, gelators **1**, **3** and **4** are able to form gels in both water and organic solvents. These results indicate that they act as versatile gelators of various solvents.

To obtain visual insights into the aggregation mode, we observed the xerogel structures prepared from their ethanol (or water) organogels by TEM. Fig. 1 shows typical images obtained from xerogels **1**–**4**. The organogel **1** forms a three-dimensional network with small 5–20 nm frizzled fibrils (Fig. 1a). On the other hand, the organogel **2** shows a straighter and larger fiber structure with 50–150 nm diameters. It should be emphasized here that many stripes can be seen in the gigantic organogel fiber when it is stained before the organogel fiber growth (Fig. 1c). The size of these stripes is comparable with that of the α-glucose-type organogel fiber. When it was stained with OsO_4 (2.0 wt%) solution after the organogel fiber growth, these stripes could not be observed (Fig. 1b). More interestingly, the α-galactose-type organogel **3** and α-mannose-type organogel **4** show spherical structures with 200–350 nm outer diameters in water (Figs. 1d and 1e), which are considered to be the aggregation of colloidal dimensions. On the other hand, **3** showed a fiber structure in ethanol (the image is not shown here). These results indicate that the morphologies of the sugar-based organogels are very dependent on gelated solvents.

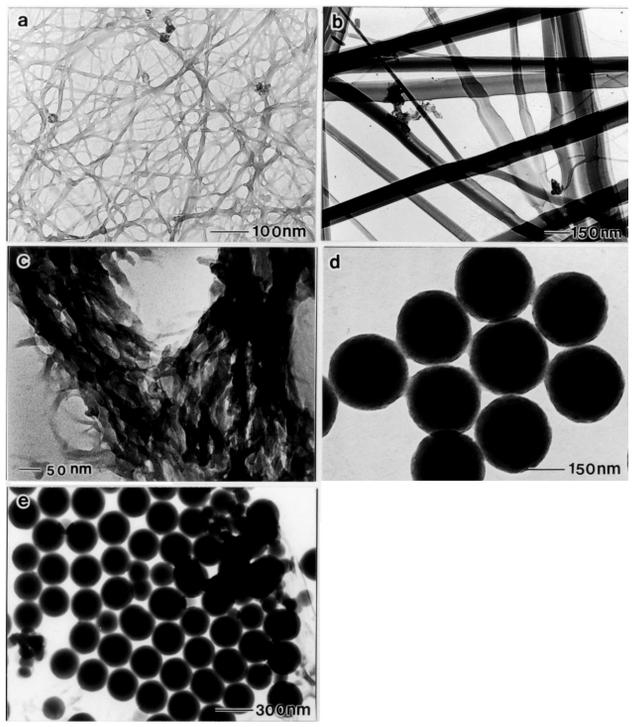

Fig. 1 TEM pictures of xerogels: (a) **1** + EtOH, (b and c) **2** + EtOH, (d) **3** + water and (e) **4** + water. In (c), the organogel was stained with OsO_4 before the organogel fiber developed.

Sol–gel polycondensation towards transcription of the organogel structures

To transcribe the superstructures formed in the organogels into the silica structure, sol–gel polycondensation of TEOS was carried out using **1**–**5** in the ethanol or water gel phase according to the method described previously.[6,7] The amino group was used in anticipation of a stronger hydrogen-bonding interaction between NH_2 and silica particles than that between NO_2 and silica particles. For instance, **1** (0.5–5.0 wt%) was dissolved in a medium for sol–gel polycondensation: the medium consists of

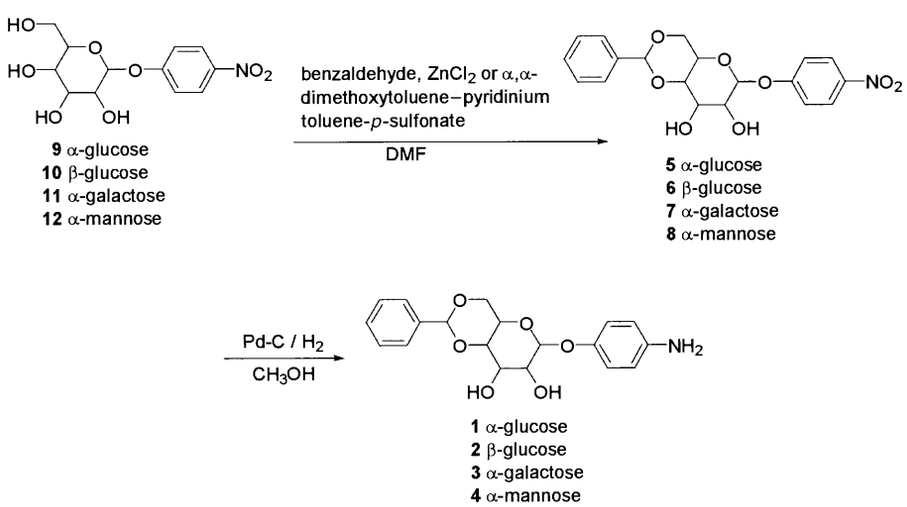

Scheme 1 Reagents and conditions for syntheses of organic gelators **1**–**4**.

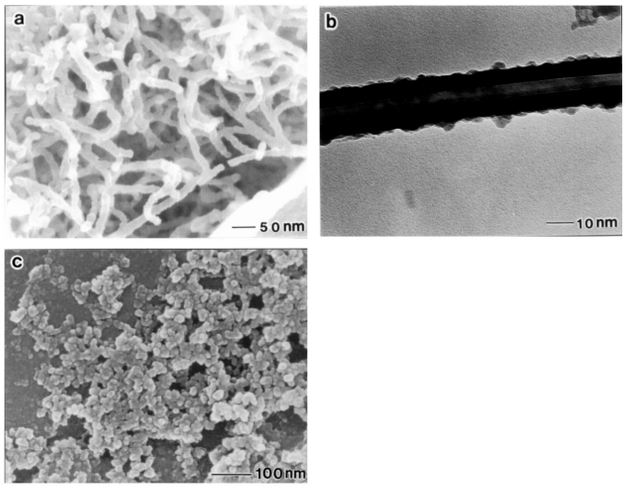

Fig. 2 (a) SEM and (b) TEM pictures of the silica obtained from ethanol organogel **1** and (c) SEM picture of the silica obtained from ethanol gel **5**.

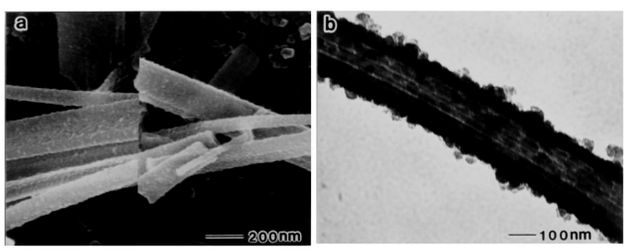

Fig. 3 (a) SEM and (b) TEM pictures of the silica obtained from ethanol organogel **2** after calcination.

ethanol or water, TEOS and benzylamine as a catalyst (for further details see the Experimental section). The sample was sealed in a glass tube and left at ambient temperature for 3–10 days. Subsequently, the samples were heated at 200 °C for 2 h and then at 500 °C for 2 h under a nitrogen atmosphere, and finally at 500 °C for 4 h under aerobic conditions. After calcination, we observed the scanning electron microscope (SEM) images of the silica materials obtained from **1** and **5** (Figs. 2a and 2c). The silica obtained from **1** shows a tubular structure with 20–30 nm outer diameters and 350–700 nm lengths whereas the silica obtained from **5** shows the conventional granular structure (Fig. 2c). It is hardly conceivable that the aromatic amino group is protonated in the presence of benzylamine. These results indicate, therefore, that the tubular structure of the silica was successfully transcribed by the hydrogen-bonding interaction between the amino group of **1** and TEOS (or oligomeric silica particles).

To further corroborate that the organogel fibers really acted as templates for the growth of the tubular silica, we took the TEM pictures after removal of **1** by calcination. The silica obtained from **1** shows an inner tube structure with 5–10 nm diameters (Fig. 2b). The inner diameter is comparable with that of the outer diameter of the fibrous organogel structure. The results again support the view that oligomeric silica particles are adsorbed onto the neutral organogel fiber by the hydrogen-bonding interaction.

In contrast, the β-glucose-type organogel **2** resulted in tubular silica with larger outer diameters of 150–200 nm (Fig. 3a). Why is the diameter of the silica obtained from organogel **2** larger than that obtained from organogel **1**? To solve this problem, we carefully took a number of TEM pictures to confirm the template effect. Very surprisingly, the TEM images of the silica obtained from **2** reveal that the silica consists of 50–100 nm inner diameters and 150–200 nm outer diameters (Fig. 3b). Furthermore, the silica in the inner tube is composed of microtubes with 5–10 nm diameters, in total giving rise to a lotus-like

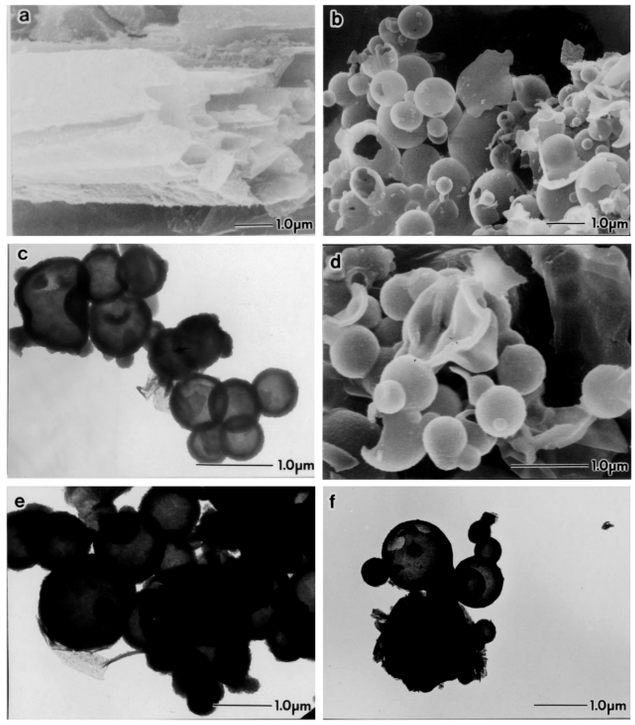

Fig. 4 SEM pictures of the silica obtained from (a) ethanol gel **3** and (b) water gel **3**, (c) TEM picture of the silica obtained from water gel **3** after calcination, (d) SEM picture of the silica obtained from water gel **4** after calcination and TEM pictures of the silica obtained from water gel **4** (e) before and (f) after calcination.

structure. The inner diameters of 5–10 nm are comparable with that of the organogel fiber obtained from **1**. We now consider, therefore, that the silica was transcribed from the hierarchical bundle structure of **2** (see Fig. 1c), because the β-glucose-type organogel **2** features a stronger intermolecular hydrogen-bonding interaction than that of the α-glucose-type organogel **1**, keeping the aggregate structure more stable.[7] This novel structure is created for the first time in the silica by transcription of bundled organogel fibers.

Fig. 4 illustrates SEM and TEM pictures of the silica materials obtained from aqueous gels **3** and **4** by sol–gel polycondensation. The silica obtained from ethanol gel **3** showed the fiber structure with *ca*. 1400 nm diameter whereas the silicas obtained from aqueous gels **3** and **4** show the spherical structure with 700–1300 nm outer diameters. Figs. 4b and 4d accidentally catch several broken particles. It is seen from these pictures that these particles have an inside cavity. Presumably, this breakage is induced during calcination to remove organic template. In addition, TEM pictures of these silica materials are displayed in Figs. 4c, 4e and 4f. All silica materials show the hollow spherical structure with 500–1000 nm inner diameters and 200–300 nm wall thickness both after and before calcination. These results indicate that the sugar-integrated gel systems can act as templates to create various new silica structures.

As a summary of the foregoing observations, we now propose a mechanism for the formation of the novel lotus-type silica structure obtained from organogel **2**, the single hollow fiber silica structure obtained from organogel **1** and the spherical silica obtained from aqueous gels **3** and **4** (Fig. 5). Oligomeric silica species are adsorbed onto the surface of the bundled fibrous structure of **2** and the polycondensation further proceeds along these bundled fibrils. This propagation mode eventually yields the lotus-type silica after combustion of gelators by calcination (Fig. 5c; lower). In contrast, **1**, **3** and **4** provide the minute fibrous and the spherical structure, respectively. Then, the tubular and the spherical silica grow by sol–gel polycondensation along these surfaces (Figs. 5b and 5c; upper and middle). As supported by correlation between the xerogel

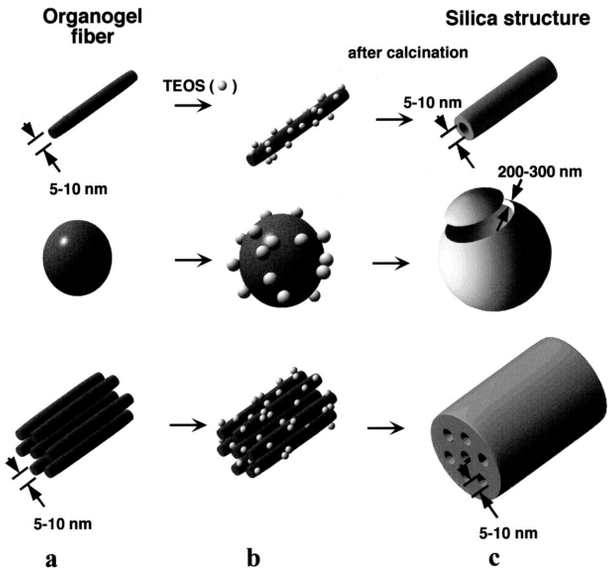

Fig. 5 Schematic representation of the creation of various silica structures from the organogel state of **1** (upper), **2** (middle) and **3** (lower) by sol–gel polymerization: (a) gelators; (b) sol–gel polymerization of TEOS and adsorption onto the gelators and (c) single hollow fiber structure (upper), spherical structure (middle) and lotus-like structure (lower) of the silica materials formed after calcination (SEM and TEM pictures in Figs. 2, 3 and 4 were taken at this stage).

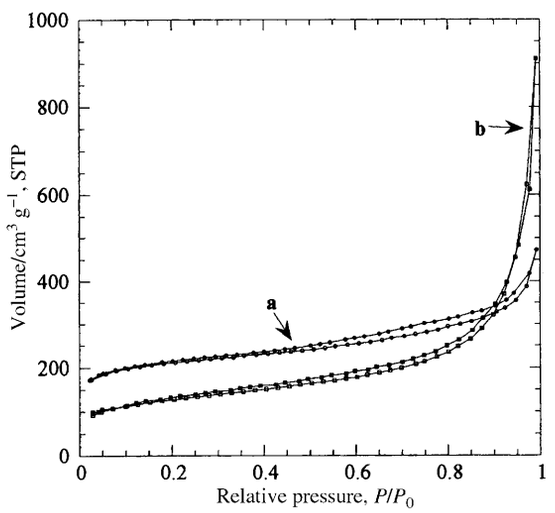

Fig. 6 Nitrogen adsorption–desorption isotherms of the silica obtained from (a) **1** and (b) **3**.

structures (Fig. 1) and the resultant silica gel structures (Figs. 2, 3 and 4), the sugar-integrated organogel structures are directly and scrupulously transcribed into the silica structures utilizing the hydrogen-bonding interactions.

Nitrogen adsorption–desorption isotherms and ^{29}Si magic angle spinning (MAS) NMR spectra of the silica

Representative nitrogen adsorption–desorption isotherms are shown in Fig. 6. The silicas obtained from ethanol gels **1** and **2** and aqueous gels **3** and **4** have a Brunauer–Emmett–Teller (BET) surface area of 450 m^2 g^{-1}, 475 m^2 g^{-1}, 650 m^2 g^{-1} and 670 m^2 g^{-1}, respectively. The surface areas of these silicas are similar to those of the silica with fibrous and lamellar structures obtained from the cholesterol organogel templates.[6c]

More important distinctions between the silica obtained from the sugar-based organogels and conventional mesoporous silica are the slightly higher degree of SiO_4 unit cross-linking in the framework and the structural stability that results from

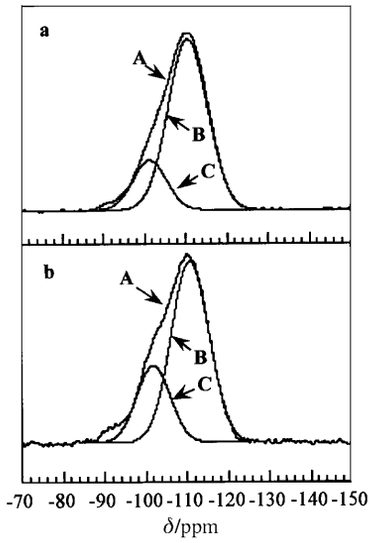

Fig. 7 ^{29}Si MAS NMR spectra of the silica obtained from (a) ethanol gel **1** and (b) aqueous gel **3**. (A) experimental curve, (B) the deconvoluted Q^4 and (C) Q^3.

this cross-linking. As shown by the deconvoluted ^{29}Si MAS NMR spectra in Fig. 7, the silica framework consists primarily of fully cross-linked Q^4 sites ($SiO–Si(OSi)_3$: with a resonance near −110 ppm) and a smaller fraction of incompletely cross-linked Q^3 sites ($HO–Si(OSi)_3$: with a resonance near −98 ppm). Generally, surfactant-containing silica mesostructures, whether assembled from ionic or neutral surfactants, exhibit Q^4/Q^3 ratios that are less than 2.0, and their calcined derivatives typically have values near 3.0.[10] However, the Q^4/Q^3 ratios for the silica materials obtained from **1**, **2**, **3** and **4** are 3.00, 3.05, 4.82 and 5.02, respectively. The Q^4/Q^3 ratios for the spherical structures of the silica are higher than those of the fiber structures of the silica obtained from organogels **1** and **2**, suggesting that the incompletely cross-linked SiOH groups may be site isolated and buried in the framework. In water, OH groups in the gelators tend to occupy the surface of the spherical structures. This molecular orientation should facilitate the formation of hydrogen bonds with SiOH groups. This interaction can be the origin of the high Q^4/Q^3 ratios.

Conclusion

The present paper has demonstrated that a variety of superstructures are conveniently obtained by self-assembling of sugar-integrated organic and aqueous gelators. Thus, a variety of superstructural silica materials such as single-fiber, lotus-like and spherical structures are created by a template method with the aid of the hydrogen-bonding interaction of the oligomeric silica species with the gelators.

In general, organic materials are capable of construction of a variety of supramolecular structures reflecting their own molecular shape, whereas such 'shape design' is very difficult from inorganic materials. The present findings suggest, as also suggested by a few other research groups, that various novel assembly structures created by weak intermolecular forces can be imprinted as permanent structures in inorganic materials. We believe, therefore, that the present system is useful for transcription of various organogel superstructures into silica materials which are eventually applicable to catalysts, memory storage, ceramic filters, *etc*.

Experimental

Equipment

^{1}H and ^{13}C NMR spectra were measured on a Bruker ARX 300 apparatus. IR spectra were obtained in KBr pellets using a

Shimadzu FT-IR 8100 spectrometer, MS spectra were obtained using a Hitachi M-250 mass spectrometer, and nitrogen adsorption–desorption isotherms were measured at 77 K by AUTOSORB-1 using standard continuous procedures (the samples were first degassed at 250 °C for 5 h). Surface areas were determined by the BET method in the 0.05–0.2 relative pressure ranges.

TEM and SEM measurements

For transmission electron microscopy (TEM) a piece of the gel was placed on a carbon-coating copper grid (400 mesh) and removed after 1 min, leaving some small patches of the gel on the grid. After specimens had been dried at low pressure, they were stained with 10 mg of OsO_4 (2.0 wt% aqueous solution). Then, they were dried for 1 h at low pressure. The specimens were examined with a Hitachi H-7100, using an accelerating voltage of 100 kV and a 16 mm working distance. Scanning electron microscopy (SEM) was taken on a Hitachi S-4500. The silica was coated with palladium–platinum and observed by 5–15 kV of the accelerating voltage and 10 μA of the emission current.

Gelation test of organic fluids

The gelator and the solvent were put in a septum-capped test tube and heated in an oil bath until the solid was dissolved. The solution was cooled at room temperature. If the stable gel was observed at this stage, it was classified as G in Table 1.

Sol–gel polycondensation of TEOS

The gelator (3–5 mg) was dissolved in water (or ethanol) (200–400 mg), and TEOS (8.0–16.0 mg), water (4.0–5.5 mg), and benzylamine (4.0–5.5 mg) were added to the gel sample and warmed until a transparent solution was obtained. The reaction mixture was placed at room temperature under the static conditions for 3–7 days. The product was dried by a vacuum pump at room temperature. Finally, the gelator was removed by calcination at 200 °C for 2 h, 500 °C for 2 h under a nitrogen atmosphere, and 500 °C for 4 h under aerobic conditions.

p-Nitrophenyl-4,6-*O*-benzylidene-α-D-glucopyranoside (5)

Compound **5** was synthesized according to the method in the literature.[7] A mixture of benzaldehyde (4.0 ml, 39.6 mmol) and *p*-nitrophenyl-α-D-glucopyranoside (1.0 g, 3.32 mmol) was stirred with zinc chloride (0.96 g, 7.08 mmol) under a nitrogen atmosphere. The reaction was continued at room temperature for 20 h. After the reaction mixture was added to water (50 ml), the solvent was decanted and the residual oil was crystallized by petroleum ether. The precipitate was collected from filtration and then purified by recrystallization (methanol). Yield 63%; mp 172.2–173.2 °C; ^{1}H NMR (300 MHz, DMSO-d_6): δ = 3.51–4.05 (m, 6H), 5.45 (d, J = 4.8 Hz, 2H), 5.52 (d, J = 6.6 Hz, 2H), 5.61 (s, 1H), 5.81 (d, J = 3.9 Hz, 1H), 7.44–7.29 (m, 7H), 8.25 (d, J = 9.3 Hz, 2H); FT-IR (KBr): ν/cm^{-1} = 3395, 2920, 1610, 1593, 1516, 1496, 1346, 1248, 1113, 1076, 997, 927, 750.

Related compounds (**6**–**8**) were synthesized by a similar method. We thus describe only their analytical data.

p-Nitrophenyl-4,6-*O*-benzylidene-β-D-glucopyranoside (6)

Yield 41%; mp 243.2–244.0 °C; ^{1}H NMR (300 MHz, DMSO-d_6): δ = 3.38–3.76 (m, 5H), 4.23 (d, J = 5.5 Hz, 1H), 5.53 (d, J = 5.1 Hz, 1H), 5.61 (s, 1H), 5.75 (d, J = 5.3 Hz, 1H), 7.29 (d, J = 9.1 Hz, 2H), 7.38–7.47 (m, 7H), 8.22 (d, J = 9.1 Hz, 2H); FT-IR (KBr): ν/cm^{-1} = 3602, 3410, 3282, 2934, 1608, 1508, 1348, 1258, 1082, 1024, 864, 752.

p-Nitrophenyl-4,6-*O*-benzylidene-α-D-galactopyranoside (7)

Yield 62%; mp 191.1–192.0 °C; ^{1}H NMR (300 MHz, DMSO-d_6): δ = 3.69–4.24 and 5.06–5.25 (m, 8H), 5.59 (s, 1H), 5.85 (d, J = 3.3 Hz, 1H), 7.31 (d, J = 8.4 Hz, 2H), 7.37–7.91 (m, 7H), 8.24 (d, J = 8.4 Hz, 2H); FT-IR (KBr): ν/cm^{-1} = 3422, 2940, 1610, 1593, 1518, 1495, 1343, 1246, 1172, 1086, 1034, 996, 924, 750.

p-Nitrophenyl-4,6-*O*-benzylidene-α-D-mannopyranoside (8)

Compound **8** was synthesized according to the literature method.[11] *p*-Nitrophenyl-α-D-mannopyranoside (500 mg, 1.66 mmol) was dissolved in dry dimethylformaldehyde (50 ml) and pyridinium toluene-*p*-sulfonate (32 mg, 0.13 mmol) was added. Benzaldehyde dimethyl acetal (303 mg, 1.99 mmol) was then added dropwise under a nitrogen atmosphere. The reaction was continued at 80 °C for 2 h. The reaction mixture was evaporated *in vacuo* to remove the solvent. The residue was purified by column chromatography on silica gel with ethyl acetate–hexane (1 : 1). Yield 70%; mp 102.2–103.2 °C; ^{1}H NMR (300 MHz, DMSO-d_6): δ = 3.49–4.02 (m, 6H), 5.26 (d, J = 6.0 Hz, 1H), 5.56 (d, J = 3.0 Hz, 1H), 5.63 (s, 1H), 5.74 (s, 1H), 7.29–7.51 (m, 7H), 8.23 (d, J = 9.0 Hz, 2H); FT-IR (KBr): ν/cm^{-1} = 432, 2932, 1610, 1593, 1518, 1495, 1344, 1247, 1095, 995, 918, 864, 752.

p-Aminophenyl-4,6-*O*-benzylidene-α-D-glucopyranoside (1)

Compound **5** (250 mg, 0.64 mmol) was dissolved in a mixture of methanol (20 ml) and THF (5 ml). Then, 10% Pd–C (25 mg) was added to the solution. Hydrogen gas was introduced into the mixed solution for 3 h at room temperature under a nitrogen atmosphere. The reaction mixture was filtered to remove Pd–C and the filtrate was evaporated *in vacuo* to dryness. The residue was purified by column chromatography on silica gel with THF–chloroform (1 : 1). Yield 40%; mp 216.7–217.0 °C; ^{1}H NMR (300 MHz, DMSO-d_6): δ = 3.44–4.10 (m, 6H), 4.76 (s, 2H), 5.25–5.31 (m, 3H), 5.60 (s, 1H), 6.70 (d, J = 9.0 Hz, 2H), 6.95 (d, J = 9.0 Hz, 2H), 7.37–7.46 (m, 5H); FT-IR (KBr): ν/cm^{-1} = 3312, 2909, 1635, 1510, 1364, 1217, 1089, 1005, 1035, 999, 806, 706; MS [3-nitrobenzyl alcohol (NBA)] *m*/*z*: 360 [M + H]$^+$; elemental analysis calcd (%) for $C_{19}H_{21}NO_6$: C 63.50, H 5.89, N 3.90; found: C 63.18, H 6.04, N 3.78%.

Related compounds (**2**–**5**) were synthesized by a similar method. We thus describe only their analytical data.

p-Aminophenyl-4,6-*O*-benzylidene-β-D-glucopyranoside (2)

Yield 44%; mp 169.6–170.1 °C; ^{1}H NMR (300 MHz, DMSO-d_6): δ = 3.40–4.21 (m, 6H), 4.71 (s, 2H), 4.82 (d, J = 4.7 Hz, 1H), 5.39 (d, J = 4.8 Hz, 1H), 5.52 (d, J = 5.3 Hz, 1H), 5.58 (s, 1H), 6.49 (d, J = 8.6 Hz, 2H), 6.76 (d, J = 8.6 Hz, 2H), 7.36–7.45 (m, 5H); FT-IR (KBr): ν/cm^{-1} = 3298, 2870, 1624, 1510, 1383, 1288, 1086, 1012, 920, 826, 771, 696; MS (NBA) *m*/*z*: 360 [M + H]$^+$; elemental analysis calcd (%) for $C_{19}H_{21}NO_6$: C 63.50, H 5.89, N 3.90; found: C 63.21, H 6.02, N 3.90%.

***p*-Aminophenyl-4,6-*O*-benzylidene-α-D-galactopyranoside (3).** Yield 62%; mp 244.1–244.3 °C; ^{1}H NMR (300 MHz, DMSO-d_6): δ = 3.78–4.68 (m, 6H), 4.71 (s, 2H), 4.87 (d, J = 6.0 Hz, 1H), 4.92 (d, J = 6.7 Hz, 1H), 5.28 (d, J = 3.4 Hz, 1H), 5.56 (s, 1H), 6.50 (d, J = 8.8 Hz, 2H), 6.79 (d, J = 8.8 Hz, 2H), 7.36–7.48 (m, 5H); FT-IR (KBr): ν/cm^{-1} = 3310, 2909, 1647, 1509, 1363, 1217, 1089, 1048, 999, 806, 763; MS (NBA), *m*/*z*: 360 [M + H]$^+$; elemental analysis calcd (%) for $C_{19}H_{21}NO_6$: C 63.50, H 5.89, N 3.90; found: C 63.26, H 5.85, N 3.83%.

***p*-Aminophenyl-4,6-*O*-benzylidene-α-D-mannopyranoside (4).** Yield 58%; mp 198.9–199.4 °C; ^{1}H NMR (300 MHz, DMSO-d_6) δ = 3.69–4.10 (m, 6H), 4.78 (s, 2H), 5.12 (d, J = 5.2 Hz, 1H), 5.21 (s, 1H), 5.32 (d, J = 4.0 Hz, 1H), 5.63 (s, 1H), 6.52 (d, J = 8.6 Hz, 2H), 6.72 (d, J = 8.6 Hz, 2H), 7.37–7.47 (m, 5H); FT-IR (KBr): ν/cm^{-1} = 3395, 3314, 2912, 1626, 1510, 1375, 1226, 1097, 1035, 926, 831, 749; MS (NBA): *m*/*z*: 360 [M + H]$^+$; elemental analysis calcd (%) for $C_{19}H_{21}NO_6$: C 63.50, H 5.89, N 3.90; found: C 63.44, H 5.89, N 3.85%.

Acknowledgements

We are grateful to the Biotechnology and Food Research Institute, Fukuoka Industrial Technology Center where we took a number of SEM and TEM pictures.

References

1 (*a*) S. Mann, *Biomimetic Materials Chemistry*, ed. S. Mann, VCH, New York, 1996; (*b*) H. Yang, N. Coombs and G. A. Ozin, *Nature*, 1997, **386**, 692; (*c*) P. Behrens and G. D. Stucky, *Angew. Chem., Int. Ed. Engl.*, 1993, **32**, 696; (*d*) F. Miyaji, S. A. Davis, J. P. H. Charmant and S. Mann, *Chem. Mater.*, 1999, **11**, 3021; (*e*) G. A. Ozin, *Chem. Commun.*, 2000, 419.

2 (*a*) D. Zhao, J. Feng, Q. Huo, N. Melosh and G. H. Fredrickson, *Science*, 1998, **279**, 548; (*b*) F. Caruso, H. Lischtenfeld, M. Giersig and H. Möhwald, *J. Am. Chem. Soc.*, 1998, **120**, 8523; (*c*) O. Velev, T. A. Jede, R. F. Lobo and A. M. Lehnoff, *Chem. Mater.*, 1998, **10**, 3597; (*d*) F. Miyaji, S. A. Davis, J. P. H. Charmant and S. Mann, *Chem. Mater.*, 1998, **10**, 3597; (*e*) Y. Ono, K. Nakashima, M. Sano, Y. Kanekiyo, K. Inoue, J. Hojo and S. Shinkai, *Chem. Commun.*, 1998, 1477; (*f*) Y. Ono, Y. Kanekiyo, K. Inoue, J. Hojo and S. Shinkai, *Chem. Lett.*, 1999, 23.

3 (*a*) K. Murata, M. Aoki, T. Suzuki, T. Harada, H. Kawabata, T. Komori, F. Ohseto, K. Ueda and S. Shinkai, *J. Am. Chem. Soc.*, 1994, **116**, 6664 and references cited therein; (*b*) T. D. James, K. Murata, T. Harada, K. Ueda and S. Shinkai, *Chem. Lett.*, 1994, 273; (*c*) S. W. Jeong, K. Murata and S. Shinkai, *Supramol. Sci.*, 1996, **3**, 83; (*d*) S. Shinkai and K. Murata, *J. Mater. Chem.*, 1998, **8**, 485; (*e*) R. Wang, C. Geiger, L. Chen, B. Swanson and D. G. Whitten, *J. Am. Chem. Soc.*, 2000, **122**, 2399; (*f*) D. C. Duncan and D. G. Whitten, *Langmuir*, 2000, **16**, 6445; (*g*) for recent comprehensive reviews, see P. Terech and R. G. Weiss, *Chem. Rev.*, 1997, 3313.

4 (*a*) K. Hanabusa, M. Yamada, M. Kimura and H. Shirai, *Angew. Chem., Int. Ed. Engl.*, 1996, **35**, 1949; (*b*) M. de Loos, J. van Esch, I. Stokroos, R. M. Kellogg and B. L. Feringa, *J. Am. Chem. Soc.*, 1997, **119**, 12675; (*c*) F. S. Schoonbeek, J. H. Esch, R. Hulst, R. M. Kellogg and B. L. Feringa, *Chem. Eur. J.*, 2000, **6**, 2633; (*d*) J. H. Esch and B. L. Feringa, *Angew. Chem., Int. Ed. Engl.*, 2000, **39**, 2263; (*e*) K. Yoza, N. Amanokura, Y. Ono, T. Akao, H. Shinmori, M. Takeuchi, S. Shinkai and D. N. Reinhoudt, *Chem. Eur. J.*, 1999, **5**, 2722.

5 (*a*) H. Nakamura and Y. Matsui, *J. Am. Chem. Soc.*, 1995, **117**, 2651; (*b*) Y. Ono, K. Nakashima, M. Sano, Y. Kanekiyo, K. Inoue, J. Hojo and S. Shinkai, *Chem. Commun.*, 1998, 1477; (*c*) J. H. Jung, Y. Ono and S. Shinkai, *Angew. Chem., Int. Ed. Engl.*, 2000, **39**, 1862; (*d*) J. H. Jung, Y. Ono and S. Shinkai, *Langmuir*, 2000, **16**, 1643; (*e*) J. H. Jung, Y. Ono and S. Shinkai, *J. Chem. Soc., Perkin Trans. 2*, 1999, 1289.

6 (*a*) J. H. Jung, Y. Ono, K. Hanabusa and S. Shinkai, *J. Am. Chem. Soc.*, 2000, **122**, 5008; (*b*) J. H. Jung, M. Amaike and S. Shinkai, *Chem. Commun.*, 2000, 2343; (*c*) J. H. Jung and S. Shinkai, *J. Chem. Soc., Perkin Trans. 2*, 2000, 2393.

7 (*a*) N. Amanokura, Y. Kanekiyo, S. Shinkai and D. N. Reinhoudt, *J. Chem. Soc., Perkin Trans. 2*, 1999, 1995; (*b*) K. Yoza, Y. Ono, K. Yoshihara, T. Akao, H. Shinmori, M. Takeuchi, S. Shinkai and D. Reinhoudt, *Chem. Commun.*, 1998, 907.

8 (*a*) R. J. H. Hafkamp, M. C. Feiters and R. J. M. Nolte, *J. Org. Chem.*, 1999, **64**, 412; (*b*) U. Beginn, S. Keinath and M. Möller, *Macromol. Chem. Phys.*, 1998, **199**, 2379.

9 (*a*) H. Yang, N. Coombs and G. A. Ozin, *Nature*, 1997, **386**, 692; (*b*) C. Boissiere, A. Larbot, A. V. D. Lee, P. J. Kooyman and E. Prouzet, *Chem. Mater.*, 2000, **12**, 2902; (*c*) J. S. Beck, J. C. Vartuli, W. J. Roth, M. E. Leonowicz, C. T. Kresage, K. D. Schmitt, C.T.-W. Chu, D. H. Olson, E. W. Sheppard and S. B. McCullen, *J. Am. Chem. Soc.*, 1992, **114**, 10834; (*d*) C. Boissere, A. V. D. Lee, A. E. Mansouri, A. Larbot and E. Prouzet, *Chem. Commun.*, 1999, 2047.

10 (*a*) P. T. Tanev, Y. Liang and T. P. Pinnavaia, *J. Am. Chem. Soc.*, 1997, **119**, 8616; (*b*) S. S. Kim, W. Zhang and T. P. Pinnavaia, *Science*, 1998, **282**, 1302.

11 J. J. Patroni, R. V. Stick, B. W. Skelton and A. H. White, *Aust. J. Chem.*, 1988, **41**, 91.